HAL
open science

Effective elastic shear stiffness of a periodic fibrous composite with non-uniform imperfect contact between the matrix and the fibers

Juan Carlos López-Realpozo, Reinaldo Rodriguez-Ramos, Raúl Guinovart-Díaz, Julián Bravo-Castillero, José A. Otero, Frederico J. Sabina, Frédéric Lebon, Serge Dumont, Igor Sevostianov

To cite this version:

Juan Carlos López-Realpozo, Reinaldo Rodriguez-Ramos, Raúl Guinovart-Díaz, Julián Bravo-Castillero, José A. Otero, et al.. Effective elastic shear stiffness of a periodic fibrous composite with non-uniform imperfect contact between the matrix and the fibers. International Journal of Solids and Structures, 2014, 51 (6), pp.1253-1262. 10.1016/j.ijsolstr.2013.12.015 . hal-01007443

HAL Id: hal-01007443

https://hal.science/hal-01007443v1

Submitted on 11 Jun 2018

HAL is a multi-disciplinary open access archive for the deposit and dissemination of scientific research documents, whether they are published or not. The documents may come from teaching and research institutions in France or abroad, or from public or private research centers.

L'archive ouverte pluridisciplinaire **HAL**, est destinée au dépôt et à la diffusion de documents scientifiques de niveau recherche, publiés ou non, émanant des établissements d'enseignement et de recherche français ou étrangers, des laboratoires publics ou privés.

Effective elastic shear stiffness of a periodic fibrous composite with non-uniform imperfect contact between the matrix and the fibers

Juan C. López-Realpozo[a], Reinaldo Rodríguez-Ramos[a], Raúl Guinovart-Díaz[a], Julián Bravo-Castillero[a], J.A. Otero[b,f], Federico J. Sabina[c], F. Lebon[d], Serge Dumont[d], Igor Sevostianov[e]

[a] Facultad de Matemática y Computación, Universidad de La Habana, San Lázaro y L, Vedado, Habana 4 CP-10400, Cuba
[b] Instituto de Cibernética, Matemática y Física (ICIMAF), Calle 15 No. 551, Entre C y D, Vedado, Habana 4 CP 10400, Cuba
[c] Instituto de Investigaciones en Matemáticas Aplicadas y en Sistemas, Universidad Nacional Autónoma de México, Apartado Postal 20-726, Delegación de Álvaro Obregón, 01000 México, DF, Mexico
[d] Laboratoire de Mécanique et d'Acoustique, Université Aix-Marseille, CNRS, Centrale Marseille, 31 Chemin Joseph-Aiguier, 13402 Marseille Cedex 20, France
[e] Department of Mechanical and Aerospace Engineering, New Mexico State University, PO Box 30001, Las Cruces, NM 88003, USA
[f] Instituto Tecnologico de Estudios Superiores de Monterrey CEM, E.M., 52926, Mexico

In this contribution, effective elastic moduli are obtained by means of the asymptotic homogenization method, for oblique two-phase fibrous periodic composites with non-uniform imperfect contact conditions at the interface. This work is an extension of previous reported results, where only the perfect contact for elastic or piezoelectric composites under imperfect spring model was considered. The constituents of the composites exhibit transversely isotropic properties. A doubly periodic parallelogram array of cylindrical inclusions under longitudinal shear is considered. The behavior of the shear elastic coefficient for different geometry arrays related to the angle of the cell is studied. As validation of the present method, some numerical examples and comparisons with theoretical results verified that the present model is efficient for the analysis of composites with presence of imperfect interface and parallelogram cell. The effect of the non uniform imperfection on the shear effective property is observed. The present method can provide benchmark results for other numerical and approximate methods.

1. Introduction

The paper addresses the problem of computation of the effective elastic properties of heterogeneous materials with imperfect bonding between the matrix and the inhomogeneities. We address the case of long fiber reinforced composite (plane strain problem and anti-plane problem). There are two ways proposed in literature to model the mentioned imperfections: (A) continuum approach when the layered inhomogeneity is considered directly and (B) discrete model when the imperfection is modeled by springs of certain stiffnesses distributed along the interface.

To the best of our knowledge, first results on inhomogeneous interface has been obtained by Kanaun and Kudriavtseva (1983, 1986) where effective elastic properties are calculated for a material containing spherical and cylindrical inhomogeneities, correspondingly, surrounded by radially inhomogeneous interphase zones. In these papers, the basic idea of replacing an inhomogeneous inclusion by an equivalent homogeneous one was formulated. Such a replacement was carried out by modeling the inhomogeneous interface by a number of thin concentric layers (piecewise constant variation of properties). The basic idea of replacing inhomogeneous inclusions by equivalent homogeneous ones has been utilized in the majority of works on the topic.

The idea of approximating radially variable properties by multiple layers (piecewise constant variation of properties) was explored by Garboczi and Bentz (1997) and Garboczi and Berryman (2000) in the context of applications to concrete composites. An alternative method was used by Wang and Jasiuk (1998). They considered a general composite material with spherical inclusions representing the interphase as a functionally graded material and calculated effective elastic moduli using the composite spheres assemblage method for the effective bulk modulus and the generalized self-consistent method for the effective shear modulus. As far as an arbitrary law of radial variation in properties is concerned, apart from the above mentioned idea of multilayer approximation, an interesting methodology was proposed by Shen and Li (2003, 2005), whereby the thickness of the interface is increased in an incremental, "differential" manner, with homogenization at each step. This idea, with modifications, has been utilized by

* Corresponding author. Tel.: +53 7 832 2466.
E-mail addresses: jclrealpozo@matcom.uh.cu (J.C. López-Realpozo), reinaldo@matcom.uh.cu (R. Rodríguez-Ramos), guino@matcom.uh.cu (R. Guinovart-Díaz), jbravo@matcom.uh.cu (J. Bravo-Castillero), jaotero@icimaf.cu (J.A. Otero), fjs@mym.iimas.unam.mx (F.J. Sabina), lebon@lma.cnrs-mrs.fr (F. Lebon), serge.dumont@u-picardie.fr (S. Dumont), igor@nmsu.edu (I. Sevostianov).

Sevostianov (2007) and Sevostianov and Kachanov (2007) for particles reinforced composites with interphase layers. The procedure of homogenization is reduced to solving non-linear ordinary differential equation.

Elastic composites with imperfect contact adherence have different area of applications. For instance, asphalt concrete (AC) is a typical multi-phase composite material. The characteristics of each constituent material in this composite and their interactions all contribute to the overall performance of the asphalt pavement, which may also be affected by the distribution and the volume fractions of these components. Particularly, these factors include the modulus and fractions of coarse aggregates and asphalt mastic which consists of asphalt and fine aggregates, air void fraction, and so on. The conventional continuum based models cannot take account of these factors in the analysis and design, and hence fail to quantitatively capture the complex mechanical behavior of the AC upon loading.

Other than the continuum approaches, micromechanical models can account for the roles of constituent materials playing in a composite. Many micromechanical-based models have been proposed to simulate the mechanical behavior of AC, for instance, see Zhu et al. (2011). However, few researchers have reported the work of the effect of the interfacial bonding strength between aggregate and asphalt mastic on the behavior of AC, which may have significant effect on the mechanical properties and failure mechanisms as well as the strengths of AC. For example, it is observed that the asphalt concrete can be easily debonded at the interface between aggregate and asphalt mastic by a fatigue loading. Craus et al. (1978) believed that the interfacial bonding strength was due to the physic-chemical reaction, which was related to the property of asphalt, geometry, size as well as surface activity of aggregate. Therefore, it is almost impossible to find a perfect interfacial bond existing between asphalt mastic and aggregates, and it may be inappropriate to describe the physical nature and macro-mechanical behavior of AC by considering the bond as the perfect kind.

An alternative approach has been, to the best of our knowledge, first proposed by Hashin (1990) who analized imperfect interface conditions in terms of linear relations between interface tractions and displacement jumps. All the thermoelastic properties of unidirectional fiber composites with such interface conditions are evaluated on the basis of a generalized self-consistent scheme model. Hashin (2002) reported that the imperfect interphase conditions are equivalent to the effect of a thin elastic interphase, and high accuracy of the method is proved by comparison of solutions of several problems in terms of the explicit presence of the interphase as a third phase. Hashin's approach was used for spherical particle-reinforced inhomogeneities by Benveniste and Miloh (2001) and Wang et al. (2005). Sevostianov et al. (2012) compared the two approaches for the case of incompressible layer between the phases and calculatee effective properties of fiber reinforced composites with periodic square arrays of fibers possessing imperfect contact with the surrounding material. They identified the interval of thickness at which the interphase does not influence the effective properties and show how the imperfection effects described by different models can be expressed in terms of each other. Guinovart-Díaz et al. (2013) used this approach for the case of a composite with parallelogram-like cell of periodicity using approach developed by Molkov and Pobedria (1985). The present work generalizes results of Guinovart-Díaz et al. (2013) to the case when the imperfectness of the contact between the matrix and the fibers is non-uniform, i.e. properties of the interface depend on both the angular and radial coordinates of a point. The aforementioned works differ to Andrianov et al. (2005, 2008) among others where homogenization method for evaluating effective properties and determining the micro-mechanical response is applied under ideal contact assumption at the interface.

2. Formulation of the problem

We consider a unidirectional periodic two-phase fiber reinforced composite shown in Fig. 1. All the fibers are assumed to be of circular cross sections with radius R. The material properties of each phase are transversely-isotropic with the axes of material and geometric symmetry being parallel. The angle of the cell θ is assumed to remain constant so that a parallelogram cell with periods w_1, w_2 can be defined. The periodicity of microstructure determines the geometry of the periodic cell S (Fig. 2). The contact between the matrix S_1 and the fibers S_2 is assumed to be non-perfect along the interface $\Gamma = \left\{z = \mathrm{Re}^{i\theta}, \quad 0 \le \theta \le 2\pi\right\}$.

In order to model various possible damages occurring on the fiber–matrix interface composite the non uniform spring formulation of imperfect bonded are considered using a generalized shear lag model (Hashin, 1990, 1991a,b), which is also called the mechanically compliant interface: tractions are assumed to be continuous across the interface while displacements may be discontinuous. The jumps in displacement components are further assumed to be proportional, in terms of the "spring-factor-type" interface parameter, to their respective interface traction component $T_3 = \sigma_{\gamma 3} n_\gamma, \quad \gamma = 1, 2$

$$T_3^{(1)} = T_3^{(2)} = \widehat{K}_s(R,\theta)\|u_3\|, \quad \text{on} \quad \Gamma. \tag{1}$$

This traction component T_3 is tangential to the interface and n is the normal unit vector to the interface Γ. $\widehat{K}_s$ is a function of the position at the interface which is called proportional interface parameter, and index "s" indicates the shear proportional spring factor. The double bar notation is used to denote the jump of the relevant function across the interphase Γ taken from the matrix (1) to the fiber (2) i.e. $\|f\| = f_1 - f_2$. The Eq. (1) is usually called a weak interface condition. It has been originally proposed by Goland and Reissner (1944) and used later in works of Benveniste and Miloh (2001), Molkov and Pobedria (1988), Mahiou and Beakou (1998), Andrianov et al. (2007).

3. Asymptotic homogenization method for the anti-plane problem

In a two-dimensional situation of uniaxially reinforced composite, the system of equations of elasticity separate in plane-strain and anti-plane-strain deformation states (see, for example, Pobedria, 1984). First of them involves in-plane displacements u_1 and u_2, while the other one, which is of particular interest in this work,

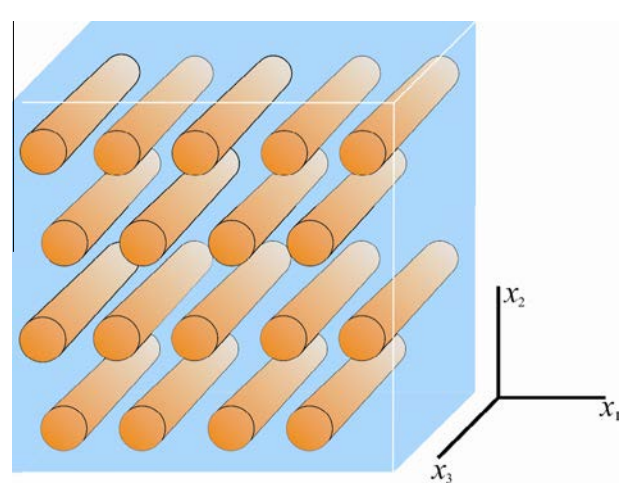

Fig. 1. The heterogeneous medium and extracted the rhombic periodic cell.

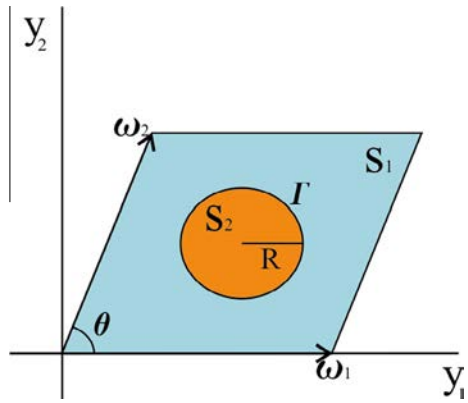

Fig. 2. The rhombic cell showing the domains S_1 and S_2 occupied by the matrix and fibers materials; Γ is the common interface.

is characterized by an out-of-plane mechanical displacement u_3 which is a function of the plane global variables x_1 and x_2. The main aim of this paper is the determination of effective properties in two-phase composites for the out-of-plane loading using the homogenization method (similarly to Lopez-Lopez et al. (2005) where the perfect bonding between the phases has been considered) accounting for mechanical imperfect conditions at the interfaces. In this case the relevant constitutive relations are

$$\sigma_{13} = 2C_{1313}\varepsilon_{13}, \quad \sigma_{23} = 2C_{2323}\varepsilon_{23} \tag{2}$$

where σ_{13}, σ_{23} are out-of-plain shear stresses, $2\varepsilon_{13} = u_{3,1}$ and $2\varepsilon_{23} = u_{3,2}$ are shear strains (comma is used to mark derivatives); and C_{1313} and C_{2323} are the elastic stiffnesses. The equilibrium equations take the form

$$\left(C_{3\gamma3\beta}(\mathbf{y})u_{3,\beta}\right)_{,\gamma} = 0, \tag{3}$$

where the Greek indices run from 1 to 2, and $\mathbf{y} = \mathbf{x}/\varepsilon$ is the local variable with $\varepsilon = l/L$ is a small geometrical parameter relating the distance l between the centers of two neighboring cylinders and L is the characteristic size of the body.

Eq. (3) has S-periodic coefficients that are rapidly oscillating. In order to obtain the homogenized equation and the corresponding effective coefficients, the solution of (3) is sought using the method of two scales by the ansatz:

$$u_3(\mathbf{x}) = v_0(\mathbf{x}) + \varepsilon v_1(\mathbf{x},\mathbf{y}) + O(\varepsilon^2), \tag{4}$$

where v_1 is a S-periodic function of y. Substituting (4) into (3), applying the chain rule considering that $\mathbf{x}$ and $\mathbf{y}$ are independent, and equating the terms of orders ε^{-1}, ε^0 to zero, one can obtain that $v_1(\mathbf{x},\mathbf{y}) = {}_{\alpha3}N(\mathbf{y})v_{0,\alpha}(\mathbf{x})$ where $v_0(\mathbf{x})$ is solution of the homogenized equation $C^*_{3\alpha3\beta}v_{0,\alpha\beta} = 0$, where $C^*_{3\alpha3\beta} = \left\langle C_{3\alpha3\beta}(\mathbf{y}) + C_{3\alpha3\delta}(\mathbf{y})_{\alpha3}N_{,\delta}(\mathbf{y})\right\rangle$ are effective coefficients. The angular brackets define the volume average per unit length over the unit cell, that is, $\langle F\rangle = \int_S F(y)dy$. The index $\alpha = 1,2$ denotes two different problems over the periodic cell which have to be solved.

The computation of the effective coefficients depends on the solution of local problems over the periodic cell in order to obtain functions ${}_{\alpha3}N(\mathbf{y})$. The solution of such local problems (called in the sequel as ${}_{\alpha3}L$) can be done using asymptotic homogenization technique (see, for instance, books of Pobedria, 1984 and Bakhvalov and Panasenko, 1989).

We focus on the so-called local (or canonical) problems associated with the correction term v_1 to the mean variations v_0 that appear in the formulae of the effective properties. There are two of such problems, which are referred as ${}_{13}L$ and ${}_{23}L$. A pre-index is used to distinguish the functions such as displacements for different local problems, which appear below.

Due to the linearity of the Eqs. (1)–(3), the correction term v_1, can be obtained as a linear combination of some of such displacements and potentials. We do not discuss it here, since the main objective of this paper is the characterization of the three effective properties $p_{11} = C^*_{1313}$, $p_{12} = C^*_{1323}$, $p_{21} = C^*_{2313}$ and $p_{22} = C^*_{2323}$. The symmetries of composite and constitutive materials lead us to find one alternative form to obtain p_{11} and p_{22} and two alternatives for obtaining $p_{12} = p_{21}$ properties as follows,

$$p_{11} = p_1V_1 + p_2V_2 + \langle p_{13}N_{,1}\rangle, \tag{5}$$

$$p_{12} = p_{21} = \langle p_{13}N_{,2}\rangle = \langle p_{23}N_{,1}\rangle, \tag{6}$$

$$p_{22} = p_1V_1 + p_2V_2 + \langle p_{23}N_{,2}\rangle, \tag{7}$$

where, $p_\gamma = C^{(\gamma)}_{1313}$ with $\gamma = 1,2$ denotes the shear moduli of matrix and fibers respectively; ${}_{13}N$ and ${}_{23}N$ are functions of $z = y_1 + y_2$ (Camacho-Montes et al., 2009) that are solutions of the local problems ${}_{13}L$ and ${}_{23}L$ respectively. $V_2 = \pi R^2/V$ and $V_1 = 1 - V_2$ are the volume fractions of matrix and fiber respectively, and $V = |w_1||w_2|\sin\theta$ is the area of periodic cell.

The mathematical statement of the problem consists to find doubly periodic functions ${}_{\alpha3}N = {}_{\alpha3}N^{(\gamma)}(\mathbf{y})$ if $\mathbf{y} \in S_\gamma$, that satisfy the following Laplace equation with the contact conditions in each phase $\gamma = 1,2$ for the local problem ${}_{\alpha3}L$ ($\alpha = 1,2$)

$$\nabla^2\,{}_{\alpha3}N^{(\gamma)} = 0, \quad \text{in} \quad S_\gamma, \tag{8}$$

imperfect contact condition

$$p_\gamma({}_{\alpha3}N^{(\gamma)}_{,1}n_1 + {}_{\alpha3}N^{(\gamma)}_{,2}n_2) + p_\gamma n_\alpha = \widehat{K}_s(\theta)\|{}_{\alpha3}N\| \quad \text{on} \quad \Gamma, \tag{9}$$

continuity condition for the stress

$$\|p_\gamma({}_{\alpha3}N^{(\gamma)}_{,1}n_1 + {}_{\alpha3}N^{(\gamma)}_{,2}n_2)\| = -\|p_\gamma\|n_\alpha, \quad \text{on} \quad \Gamma, \tag{10}$$

$$\langle {}_{\alpha3}N\rangle = 0, \ \text{in}\ S = S_1 \cup S_2, \tag{11}$$

$\mathbf{n} = (n_1, n_2)$, is the outward unit normal vector to the interface Γ and the proportional interface parameter depends on the angle θ only for a fixed fiber volume fraction, and $p_\gamma = C^{(\gamma)}_{1313}$ with $\gamma = 1,2$ is the shear moduli of the matrix and fibers. The pre-index used in (8)–(11) for the local function will be omitted hereafter. The problem (8)–(11) should be converted into dimensionless problems using the dimensionless variable $\xi = y/l$ (this is not a small parameter!), then $N^{(\gamma)}_{,i} = u^{(\gamma)}_{,i}$ and $N^{(\gamma)}_{,ii} = u^{(\gamma)}_{,ii}/l$ where $u^{(\gamma)} = N^{(\gamma)}/l$ and the derivative $u_{,i}$ is with respect to the variable ξ_i and $u_3 \equiv u$. The interface parameter is replaced by $\widehat{K}_s = K_s p_1/R_0$, K_s is a dimensionless parameter and R_0 is the true radius of the fibers in the composite. Also the dimensionless parameter $R = R_0/l$ is introduced. The dimensionless problem related to (8)–(11) over the periodic cell Y are now rewritten below Laplace equation

$$\nabla^2 u^{(\gamma)} = 0, \ \text{in}\ S_\gamma, \tag{12}$$

imperfect contact condition

$$\frac{p_\gamma(u^{(\gamma)}_{,1}n_1 + u^{(\gamma)}_{,2}n_2) + p_\gamma n_\alpha}{p_1} = \frac{K_s(\theta)}{R}\|u\|, \ \text{on}\ \Gamma, \tag{13}$$

continuity condition for the stress

$$\left\|\frac{p_\gamma(u^{(\gamma)}_{,1}n_1 + u^{(\gamma)}_{,2}n_2)}{p_1}\right\| = -(1-\kappa)n_\alpha, \ \text{on}\ \Gamma, \tag{14}$$

$$\langle u\rangle = 0, \quad \text{in} \quad S = S_1 \cup S_2, \tag{15}$$

where $\kappa = p_2/p_1$ and $u = u^{(\gamma)}$ if $\xi \in S_\gamma$.

4. Solution of local problems with non-uniform imperfect spring parameters

The well-developed theory of analytical functions (Muskhelishvili, 1953) can be used to solve the problem (12)–(15). Thus, it is necessary to solve the local problems ${}_{\alpha 3}L$. Doubly periodic harmonic functions in the matrix ($\gamma = 1$) and fiber ($\gamma = 2$) region are to be found for the ${}_{\alpha 3}L$ local problems in terms of harmonic functions $\varphi_\gamma(z)$

$$u^{(\gamma)} = \mathrm{Re}\left\{\varphi_\gamma(z)\right\}. \tag{16}$$

Now, we consider a partition of the interface $\Gamma = \cup\Gamma_j,\ \Gamma_i \cap \Gamma_j = \emptyset,\quad i \neq j$ by n arcs, where a piecewise constant function $K_s(\theta) = K_j,\quad \theta_j < \theta < \theta_{j+1}$ with $j = 0, ..., n-1,\quad \theta_0 \equiv 0,$ $\theta_n \equiv 2\pi$ is assumed and θ_j denotes the angle of each arc (Fig. 3).

In each arc of the interface Γ we consider

$$\begin{aligned} \varphi_1^j &= \frac{a_0^j z}{R} + \sum_{k=1}^{\infty}{}^{o} \left.\frac{\zeta^{(k-1)}(z/R)}{(k-1)!}\right) a_k^j \text{ and} \\ \varphi_2^j(z) &= \sum_{p=1}^{\infty}{}^{o} \left(\frac{z}{R}\right)^p c_p^j, \quad |z| = \mathrm{R}e^{i\theta} \end{aligned} \tag{17}$$

$\zeta(z)$ is the Weierstrass's quasi periodic Zeta function defined as $\zeta(z) = \frac{1}{z} + \sum_{m,n}{}' \left(\frac{1}{z - P_{nm}} + \frac{1}{P_{nm}} + \frac{z}{P_{nm}^2}\right),\ P_{nm} = nw_1 + mw_2,$ for $m,\ n \in Z,$ and the prime over the summation symbol means that the pair $(m,n) = (0,0)$ is excluded. The Laurent's expansion of function $\varphi_1^j(z)$ is given by the following expression

$$\varphi_1^j(z) = \frac{z}{R} a_0^j + \sum_{p=1}^{\infty}{}^{o} \left(\frac{R}{z}\right)^p a_p^j - \sum_{p=1}^{\infty}{}^{o} \sum_{k=1}^{\infty}{}^{o} \left(\frac{z}{R}\right)^p \sqrt{\frac{k}{p}} w_{kp} a_k^j, \tag{18}$$

where $w_{kp} = \frac{(k+p-1)!}{(k-1)(p-1)!} \frac{S_{k+p} R^{k+p}}{\sqrt{kp}},\quad S_{k+p} = \sum_{m,n} (mw_1 + nw_2)^{-(k+p)},$ $m^2 + n^2 \neq 0,\ k + p \geqslant 2,\ S_2 = 0$. The constants $a_0^j,\ a_p^j,\ c_p^j$ and $z = \xi_1 + i\xi_2$ are complex numbers; the over bar indicate complex conjugate and the superscript "o" on the summation indicates that the sum is carried out only over odd indices, w_1, w_2 are the periods and $a_0^j = -R^2 H_1 \overline{a}_1^j - R^2 H_2 a_1^j$, where $H_1 = \frac{\overline{\delta}_1 \overline{w}_2 - \overline{\delta}_2 \overline{w}_1}{w_1 \overline{w}_2 - w_2 \overline{w}_1}, H_2 = \frac{\delta_1 \overline{w}_2 - \delta_2 \overline{w}_1}{w_1 \overline{w}_2 - w_2 \overline{w}_1}$, with $\delta_i = \zeta(z + w_i) - \zeta(z)$.

Replacing (16)–(18) into (13), and (14) and after some algebraic manipulations, the following system of equations is obtained in order to find the complex unknown coefficients a_k^j for each arc by the system

$$\begin{aligned} &\overline{a}_p^j + \beta_1^j R^2 H_1 \delta_{1p} \overline{a}_1^j + \beta_1^j R^2 H_2 \delta_{1p} a_1^j + \beta_p^j \sum_{k=1}^{\infty}{}^{o} w_{kp} a_k^j \\ &\quad = \beta_1^j \delta_{1p} (\delta_{1\alpha} - i\delta_{2\alpha}) R, \end{aligned} \tag{19}$$

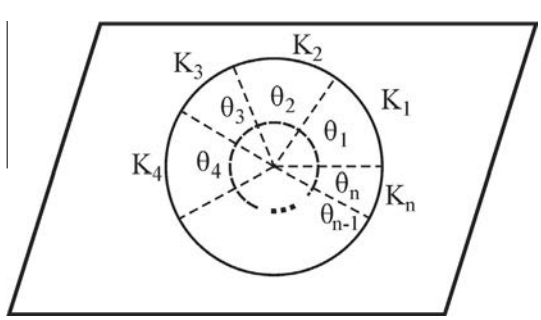

Fig. 3. Partition of the interface in n arcs.

only survives where δ_{kp} is the Kroneckefs delta and $\beta_p^j = \frac{K_j(1-\kappa)+\kappa p}{K_j(1+\kappa)+\kappa p}$ and K_j is the tangential component of the imperfect parameter for each arc. Details of the derivation of (19) are given in Appendix A. The series $\sum_{k,p=1}^{\infty}{}^{o} |w_{kp}|$ is convergent and consequently the system (19) is a normal infinity system of algebraic equations (see, for instance, Kantarovich and Krylov, 1964) which could be truncated in order to obtain approximations of the undetermined constants a_k^j. In order to find the solution of the system (19), the latter is reduced to two subsystems with real and imaginary separated parts. The magnitudes $a_k = x_k + iy_k,\ H_\gamma = h_{1\gamma} + ih_{2\gamma},\ w_{kp} = w_{1kp} + iw_{2kp}$ where x_k, y_k, $h_{1\gamma}$, $h_{2\gamma}$, w_{1kp}, and w_{2kp} are real numbers, represent the real or imaginary parts of complex numbers a_k, β_p, H_1, H_2, w_{kp} respectively.

The system (19) for $p = 1$ in each arc is written in matricial compact form as follows

$$\left(I + \beta_1^j R^2 J\right) X^j + \beta_1^j N_1 X_1^j = R_1 \beta_1^j B, \tag{20}$$

where I represents the 2×2-unit matrix, J is the square matrix defined by $J = \begin{pmatrix} (h_{11} + h_{12}) & (h_{21} - h_{22}) \\ (-h_{21} - h_{22}) & (h_{11} - h_{12}) \end{pmatrix}$, the infinite matrix $N_1(n_{k1})$ is composed by two rows or horizontal square blocks of order 2 of the form $n_{k1} = \begin{pmatrix} w_{1k1} & -w_{2k1} \\ -w_{2k1} & -w_{1k1} \end{pmatrix}$, k = 2s + 1. Moreover, the transpose vectors of unknowns $X_1^T = (x_1, y_1)$, $B^T = (\delta_{1\alpha}, \delta_{2\alpha})$ and $X^T = (x_3, y_3, \ldots, x_k, y_k, \ldots)$ are given.

The system (19) for $p \geq 3$ in each arc is transformed into

$$(I + W) X_2^j = -N_2 X_1^j \tag{21}$$

where the matrix W = W(nkp) is composed by square blocks of order 2 of the form $n_{kp} = \chi_p \begin{pmatrix} w_{1kp} & -w_{2kp} \\ -w_{2kp} & -w_{1kp} \end{pmatrix}$, k = 2s + 1, p = 2t + 1, s = t = 1, 2, 3, ... and $N_2 = N_2(n_{1p})$ is formed by two columns or vertical square blocks of order 2. From (21) follows $X_2^j = -(I + W)^{-1} N_2 X_1^j$ and substituting into (20) results

$$a_1^j = (1, i) R \left(I + \beta_1^j R^2 J - \beta_1^j N_1 (I + W)^{-1} N_2\right)^{-1} B. \tag{22}$$

In order to determine the effective properties, it is necessary to truncate the system of Eq. (19) into an appropriate order $k = p = N_0$. A very important first approximation is obtained if we consider $N_0 = 1$, in this case only survives the unknowns with subscripts $k = 1$ for the system (19). It is easy to solve this system and its solution is

$$\begin{pmatrix} x_1^j \\ y_1^j \end{pmatrix} = R\left(I + \beta_1^j R^2 J\right)^{-1} B. \tag{23}$$

Introducing the notation for each arc in the form

$$Z^j = I + \beta_1^j R^2 J - \beta_1^j N_1 (I + W)^{-1} N_2, \tag{24}$$

the following explicit expressions of a_1^j are obtained from (22) for the local problems ${}_{13}L$ and ${}_{23}L$ respectively

$${}_{13}a_1^j = R\beta_1^j (z_{22} - iz_{21}) / |Z^j| \tag{25}$$

$${}_{23}a_1^j = -\left(R\beta_1^j (z_{12} - iz_{11})\right) / |Z^j| \tag{26}$$

where $|Z^j|$ denotes the determinant of numerical symmetric matrix Z.

5. Effect of non-uniform imperfect spring parameters on overall properties

Eqs. (5)–(7) can be easily transformed to the area integrals applying Greeńs theorem. Replacing $N^{(\gamma)} = u^{(\gamma)}/l$, $dy_i = ld\xi_i$, the effective coefficients p_{11}, p_{12}, p_{21} and p_{22} are connected by the following relations

$$p_{11} - ip_{21} = p_1V_1 + p_2V_2 - \frac{p_1}{V}\left(i\int_\Gamma u^{(1)}d\xi_1 + \int_\Gamma u^{(1)}d\xi_2\right) + \frac{p_2}{V}\left(i\int_\Gamma u^{(2)}d\xi_1 + \int_\Gamma u^{(2)}d\xi_2\right), \tag{27}$$

$$p_{12} - ip_{22} = -i(p_2V_1 + p_2V) - \frac{p_1}{V}\left(i\int_\Gamma u^{(1)}d\xi_1 + \int_\Gamma u^{(1)}d\xi_2\right) + \frac{p_2}{V}\left(i\int_\Gamma u^{(2)}d\xi_1 + \int_\Gamma u^{(2)}d\xi_2\right), \tag{28}$$

where V_1 and $V_2 = \pi R^2/V$ are the volume fractions of matrix and inclusion respectively, $V_1 + V_2 = 1$ and $V = |w_1||w_2|\sin\theta$ denotes the volume of the parallelogram periodic cell. In (27) $u^{(\gamma)}$ is the solution of the local problem ${}_{13}L$ whereas in (28) $u^{(\gamma)}$ is the solution of the ${}_{23}L$. Taking into account (16)–(18) the analytical formulae for effective properties are deduced from (27) and (28) depending on a_1^j as follows

$$p_{11} - ip_{21} = p_1\left[1 - \frac{V_2}{\pi R}\sum_{j=0}^{n-1}{}_{13}\overline{a}_1^{j+1}\left(\theta_{j+1} - \theta_j\right)\right] - \frac{p_1V_2}{\pi R}\sum_{j=0}^{n-1}\left\{\begin{array}{l}\displaystyle\sum_{p=1}^{\infty}{}^{o}e^{-\frac{i(p+1)\left(\theta_j+\theta_{j+1}\right)}{2}}\frac{}{p+1}\mathrm{sen}\left[\frac{(p+1)\left(\theta_{j+1}-\theta_j\right)}{2}\right]\left[2_{13}a_p^{j+1} - (1-\kappa)\delta_{1p}R\right] \\ \displaystyle +2\sum_{p=3}^{\infty}{}^{o}{}_{13}\overline{a}_p^{j+1}\frac{e^{\frac{i(p-1)\left(\theta_{j+1}+\theta_j\right)}{2}}}{p-1}\mathrm{sen}\left[\frac{(p-1)\left(\theta_{j+1}-\theta_j\right)}{2}\right]\end{array}\right\} \tag{29}$$

$$p_{12} - ip_{22} = -p_1\left[i + \frac{V_2}{\pi R}\sum_{j=0}^{n-1}{}_{23}\overline{a}_1^{j+1}\left(\theta_{j+1} - \theta_j\right)\right] - \frac{p_1V_2}{\pi R}\sum_{j=0}^{n-1}\left\{\begin{array}{l}\displaystyle\sum_{p=1}^{\infty}{}^{o}e^{-\frac{i(p+1)\left(\theta_j+\theta_{j+1}\right)}{2}}\frac{}{p+1}\mathrm{sen}\left[\frac{(p+1)\left(\theta_{j+1}-\theta_j\right)}{2}\right]\left[2_{23}a_p^{j+1} + i(1-\kappa)\delta_{1p}R\right] \\ \displaystyle +2\sum_{p=3}^{\infty}{}^{o}{}_{23}\overline{a}_p^{j+1}\frac{e^{\frac{i(p-1)\left(\theta_j+\theta_{j+1}\right)}{2}}}{p-1}\mathrm{sen}\left[\frac{(p-1)\left(\theta_{j+1}-\theta_j\right)}{2}\right]\end{array}\right\} \tag{30}$$

where a_1^j in (29), (30) are given by (25), and (26), respectively. Details in the derivation of the effective coefficients (29), and (30) are given in Appendix B.

The analytical expressions of effective properties (29), and (30) are functions of the properties and volume fractions of constituents, of periodic cell w_1, w_2 and the imperfect parameters K_j in each arc. The effective properties of a composite with perfect adhesion between the constituents are obtained from (29), and (30) taking $K_1 = K_2 = K_3 = \ldots K_j = K \to \infty$ and the total separation occurs when $K_1 = K_2 = K_3 = \ldots K_j = K \to 0$. From the symmetric matrix Z^j is deduced $p_{12} = p_{21}$. The effective coefficients p_{11}, p_{22} and $p_{12} = p_{21}$ represent the effective axial coefficients of an orthotropic fiber reinforced composite with defect at the interface Γ.

Once solved (19), the series expansion (17) depend on the contrast between the properties of the components and on the volume fraction of the fibres. In the case of a high-contrast composite with densely-packed fibres, the gradients of the local fields can grow significantly. Then, the convergence of the series decreases and evaluation of the accurate numerical results may become very time-consuming. In this sense, the above computations were made for $N_0 = 10$, where N_0 denotes the number of equations considered in the solution of the infinite algebraic system of Eq. (19). The solution to the infinite order algebraic system (19) is achieved by means of truncation to an infinite order and the Cramer's rule. A fast convergence of successive truncations is ensured because the system is regular (see references in Rodriguez-Ramos et al. (2001)) so that successive approximations can be applied. In general, for low volume fraction of fiber ($V_2 < 0.4$) the accuracy and convergence of the results are good for much smaller values of N_0 ($N_0 \leqslant 2$). More terms are required for high volume fraction of fibers as well as high contrast of fiber and matrix, in particular, $N_0 > 10$ gives an approximation with absolute error less than 1%. The absolute error between two consecutive truncations is very low.

The explicit analytical form of the effective coefficients (29), and (30) are large and complicated. They require computation of a number of terms of series (17) and the solution of the system (19). However, once the computational program is established the time-consuming is very short.

6. Results and discussion

We now illustrate the theory with several examples. First, as a validation of the model we consider different particular cases for a two phase composites with various geometries of the periodic cell. From now on, we will use the two-index notation for the elastic constants.

Actually, it makes sense to mention that although the method is not for dilute approximation (Movchan et al., 2002) it works perfect for volume fraction of inhomogeneities up to 50% as it was checked by Sevostianov et al. (2006), Sevostianov and Sabina (2007).

6.1. In Tables 1 and 2 a comparison between the model reported by Jiang et al. (2004) and the present model is given. Table 1 presents the normalized effective elastic moduli $C_{44}^*/C_{44}^{(1)}$, $C_{45}^*/C_{44}^{(1)}$, $C_{55}^*/C_{44}^{(1)}$ for perfect contact ($K = 10^{12}$) computed by AHM and the results reported in Table 4 of Jiang et al. (2004). The material parameter used for this calculation is $C_{44}^{(2)}/C_{44}^{(1)} = 120$ and the angle of the periodic cell is $\theta = 75°$. Table 2 shows the behavior of the effective longitudinal shear elastic moduli C_{44}^*, C_{55}^* for a porous material with the shear modulus of the matrix $C_{44}^{(1)} = 30$GPa.

The uniform imperfect elastic spring contact are obtained as a particular case of this work taking $K_1 = K_2 = K_3 = \ldots K_j = K$ with $0 < K < \infty$. Now, some comparisons with other theoretical approaches are given in order to validate the imperfect uniform model. Table 3 illustrates the normalized effective elastic moduli $C_{44}^*/C_{44}^{(1)}$, $C_{45}^*/C_{44}^{(1)}$, and $C_{55}^*/C_{44}^{(1)}$ for two types of imperfect uniform contact ($K = 10^{-5}$, $K = 10$) computed by the present model and the results reported by Lopez-Realpozo et al. (2011). The material parameter used for this calculation is $C_{44}^{(2)}/C_{44}^{(1)} = 120$ and the angle of the periodic cell is $\theta = 45°$.

6.2. In order to show the novelty of this work, we consider the non-uniform imperfect contact for two phase composites with square cell. The material parameters used is $C_{44}^{(2)}/C_{44}^{(1)} = 120$. We consider the interface of the two phase composite divided into two pieces $\Gamma = \Gamma_1 \cup \Gamma_2$ and different spring imperfect parameter constants K_1 and K_2 are assigned on Γ_1 and Γ_2 respectively,

Table 1
Effective elastic moduli obtained by Jiang et al. (2004) and AHM for perfect contact and periodic cell with angle $\theta = 75^o$ $\left(C_{44}^{(2)}/C_{44}^{(1)} = 120\right)$.

V_2	$C_{44}^*/C_{44}^{(1)}$		$C_{45}^*/C_{44}^{(1)}$		$C_{55}^*/C_{44}^{(1)}$	
	Jiang et al.	AHM	Jiang et al.	AHM	Jiang et al.	AHM
0.10	1.21780	1.21780	0.00133	0.00133	1.21852	1.21852
0.20	1.48816	1.48816	0.00672	0.00672	1.49176	1.49176
0.30	1.83374	1.83374	0.01968	0.01968	1.84428	1.84428
0.40	2.29477	2.29477	0.04739	0.04739	2.32016	2.32016
0.50	2.95203	2.95203	0.10602	0.10602	3.00884	3.00884
0.60	4.00126	4.00123	0.23812	0.23812	4.12884	4.12884

Table 2
Variations of effective longitudinal shear elastic modulus for a porous material with $C_{44}^{(1)} = 30$GPa.

V_2	$C_{44}^* = C_{55}^*$			
	Square cell ($\theta = 90°$)		Hexagonal cell ($\theta = 60°$)	
	Jiang et al.	AHM	Jiang et al.	AHM
0.00	30.00000	30.00000	30.00000	30.00000
0.10	24.54550	24.54545	24.54530	24.54530
0.20	20.00000	19.99996	19.99590	19.99592
0.30	16.15330	16.15326	16.12740	16.12740
0.40	12.85340	12.85336	12.76050	12.76054
0.50	9.98430	9.98427	9.73960	9.73964
0.60	7.45030	7.45029	6.90960	6.90954

according to the following distribution function $K_s(\theta) = \begin{cases} K_1, & 0 \le \theta < \theta_1, \\ K_2, & \theta_1 \le \theta \le 2\pi. \end{cases}$ (see Fig. 3). Different cases of imperfection spring parameters are considered. A wide range of situations could be taken into account but only the cases of imperfect parameters given in Fig. 4 are chosen. The perfect case ($K_1 = K_2 = 10^{12}$) and empty fibers ($K_1 = K_2 = 10^{-12}$) are upper and lower bounds of the remaining imperfect situations for the effective coefficient $C_{44}^* = C_{55}^*$. Moreover, it is well known that for composites with square cell the effective coefficient C_{45}^* is zero. However, the non-uniform spring distribution strongly affects the anisotropic character of the composite, making the effective coefficient C_{45}^* different from zero. The curves indicate an irregular behavior for the coefficient C_{45}^* where it is zero for perfect and void cases and the behavior of this coefficient is strictly increasing for $K_1 = 10^{12}, K_2 = 0$ making this property in the composite stiffer whereas the remaining cases are strictly decreasing, therefore, the property is softer.

6.3. Fig. 5 illustrates the comparison of the axial effective properties of fibrous composite for two different periodic cells, square ($\theta = 90°$) and rhombic ($\theta = 45°$) cells vs. the fiber volume fraction. The composite has non uniform imperfection at the interface Γ and the partition of the interface is given in two arcs $[0, 90°]$ and $[90°, 360°]$, with different lengths where two sets of piecewise constant functions take the values $K_1 = 1$ and $K_2 = 50$, (solid line) and $K_1 = 50$, $K_2 = 1$ (dashdot) on the arcs, respectively. The material contrast is $\kappa = p_2/p_1 = 120$. The behavior of the effective property C_{55}^* is affected for square or rhombic cell and the coefficient C_{55}^* changes considerable under non-uniform adherence of the composite as well. Besides, the configuration of the cell strong influences on the property of the composite C_{45}^* where the curves reflect the difference between square and rhombic cells. Moreover, in recent contributions of Rodriguez-Ramos et al. (2011, 2012) and Guinovart-Díaz et al. (2012) are pointed out that the configuration of the cell affects the anisotropic properties of elastic and piezoelectric composites. For example, composites with periodic cell

Table 3
Effective elastic moduli obtained by Lopez-Realpozo et al. (2011) and present model for uniform imperfect contact and periodic cell with angle $\theta = 45°$. Ratio between the constituent properties is $C_{44}^{(2)}/C_{44}^{(1)} = 120$.

K	V_2	$C_{44}^*/C_{44}^{(1)}$		$C_{45}^*/C_{44}^{(1)}$		$C_{55}^*/C_{44}^{(1)}$	
		IJMS 2011	Present model	IJMS 2011	Present model	IJMS 2011	Present model
10^{-5}	0.1	0.821	0.821	−0.003	−0.003	0.815	0.815
	0.4	0.455	0.455	−0.033	−0.033	0.389	0.389
10	0.1	1.178	1.178	−0.003	−0.003	1.172	1.172
	0.4	2.062	2.062	−0.091	−0.091	1.879	1.879

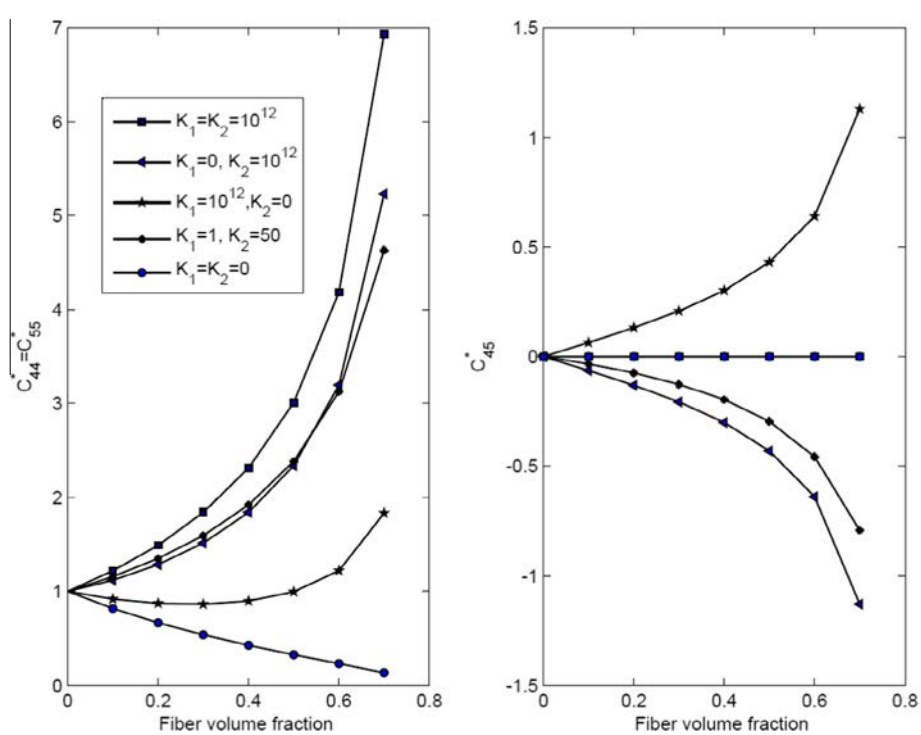

Fig. 4. Behavior of antiplane effective coefficients for two phase composite with non-uniform imperfect contact.

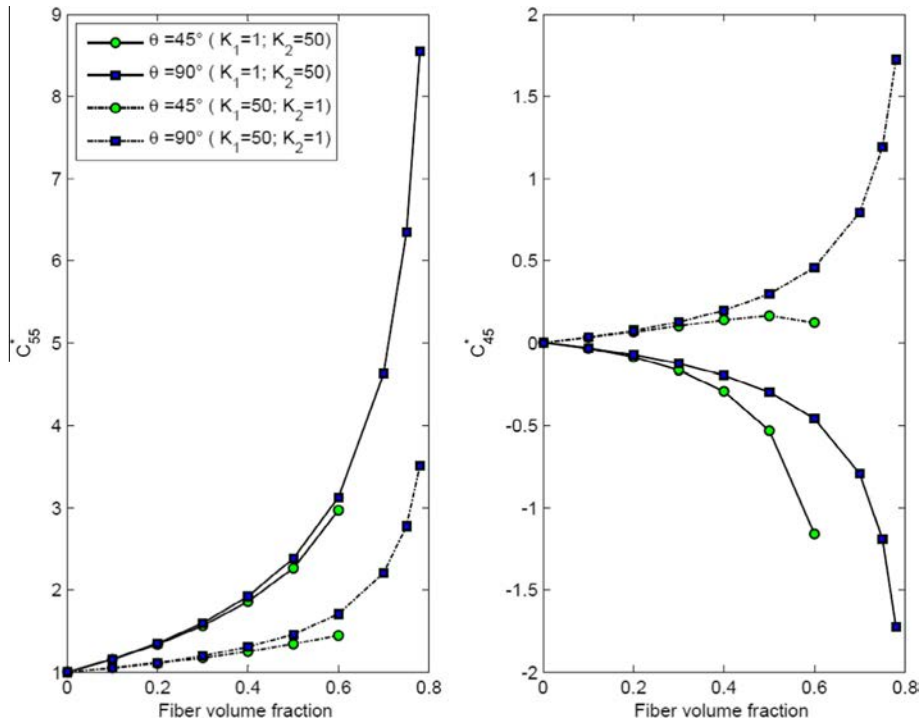

Fig. 5. Axial effective properties of fibrous composite for two different periodic cells, square and rhombic cells and two different non uniform spring imperfections ($K_1 = 1$ and $K_2 = 50$; $K_1 = 50$ and $K_2 = 1$) at the interface Γ.

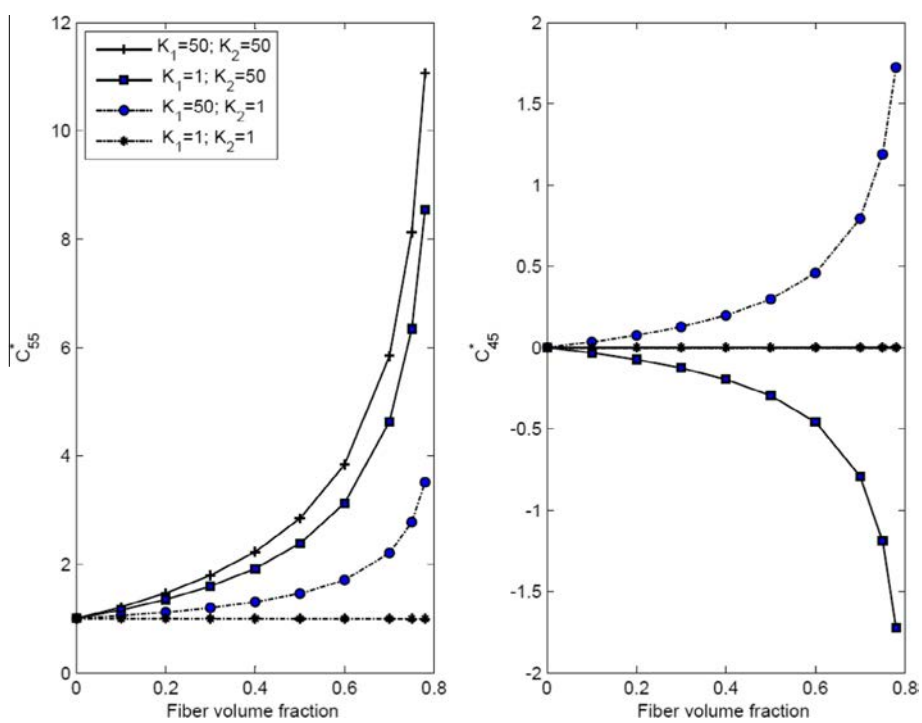

Fig. 6. Axial effective properties of fibrous composite for square periodic cell with uniform and non-uniform contacts.

$\theta = 45^\circ$ (the effective coefficient C^*_{45} is different from zero) in general has monoclinic symmetry which is different to composites with configuration of square ($\theta = 90^\circ$) cell (the effective coefficient C^*_{45} is equal to zero) where the symmetry group is 4 mm. But in this work is shown the relevant influence of the non-uniform imperfect contact, which makes the same property C^*_{45} different from zero for square cell. The small value of imperfect parameters K_i indicates a major weakening of interactions at the interface. As was to be expected, when to the arc $[90^\circ, 360^\circ]$ of major length corresponds the minor value $K_2 = 1$ the effective properties C^*_{55} is weaker without regards to the periodic cell. In the same case, the effective coefficient C^*_{45} is positive and in the other case is positive. Notice the symmetry respect to horizontal axis of C^*_{45} for square cell and the other case.

6.4. Finally, the behavior between the uniform and non-uniform imperfect interfaces is illustrated in Fig. 6. Notice that the behavior

of the axial effective properties of fibrous composite for square periodic cell change considerable in composites with uniform and non-uniform imperfect contacts. In this case, for the effective property C^*_{55} the uniform imperfect adherence $K_1 = K_2 = 1$ and $K_1 = K_2 = 50$ in the composite are lower and upper bounds respectively of the curves for non uniform imperfections. The effective property C^*_{45} is zero for uniform imperfect contact in composites with square periodic cell but the anisotropic is affected and for that reason this effective coefficient is different from zero.

7. Conclusions

An asymptotic homogenization technique is used for calculation effective shear moduli of an elastic fiber reinforced composite with non-uniform imperfect bonding between constituents and parallelogram periodic cell. We introduce different elastic *spring* constants for each partition of the interface Γ, between the matrix and inclusions, where a piecewise constant function $K_s(\theta) = K_j$, $\theta_j < \theta < \theta_{j+1}$ transmits a load from the matrix to the inclusion; the transmission stress is proportional to the displacement jump across the "matrix-inclusion" interface. Simple analytical expressions (29), and (30) of the shear moduli using asymptotic homogenization approach are derived that show the anisotropic response of the composite. In the asymptotic limit, we can simulate different degrees of the interface's response: (i) the case of the perfect bonding $K_1 = K_2 = K_3 = \ldots K_j = K \to \infty$, (ii) the case of the complete separation $K_1 = K_2 = K_3 = \ldots K_j = K \to 0$ of the matrix and fibers, (iii) the influence of one part of imperfect contact with respect to the other one in the whole composite where the interface Γ is partitioned. The non-uniform imperfect interface and the angle of inclination of the cell play an important role in the global behavior of the composite. The accuracies of the solutions were tested with other theoretical models and experimental data and good agreement were observed. Since the derived semi-analytic formulae are not constrained in the whole range of fiber volume fraction, enough good numerical results up to percolation limit are obtained. These models can be extended to more complex composites in order to predict the overall properties in the design and manufacturing of one-directional fibrous composite materials.

Acknowledgments

The funding of CONACYT project number 129658 and Proyecto Nacional de Ciencias Basicas 2013-2014 are gratefully acknowledged. The authors acknowledge to the project SHICHAN, supported by FSP (Cooperation Scientifique Franco-Cubaine) Cuba 2011-26, No. 29935XH. Thanks to Departamento de Matemáticas y Mecánica IIMAS-UNAM for their support and Ramiro Chávez Tovar and Ana Pérez Arteaga for computational assistance.

Appendix A.

Derivation of the system given by (19)

The problem (12)–(15) is solved for both antiplane problem $L_{\alpha 3}$ with $\alpha = 1, 2$. Using the imperfect contact conditions spring type (13), the continuity condition for the stress (14) and taking into account $C^{(1)}_{55} = C^{(1)}_{44} = C^{(1)}_{\alpha 3 \alpha 3}$ and $\kappa = \frac{p_2}{p_1} = \frac{C^{(2)}_{55}}{C^{(1)}_{55}}$ we obtain

$$\left[({}^j u_{,1}^{(1)} n_1 + {}^j u_{,2}^{(1)} n_2) - \kappa({}^j u_{,1}^{2} n_1 + {}^j u_{,2}^{(2)} n_2) + (1-\kappa)(\delta_{1\alpha} n_1 + \delta_{2\alpha} n_2)\right]_\Gamma = 0 \tag{31}$$

The function ${}^j u$ is considered for the matrix and fiber as a function of complex variable, i.e.

$${}^j u_{(1)} = {}^j u_1 + {}^j u_2 i, \quad {}^j u_{(2)} = {}^j v_1 + {}^j v_2 i, \tag{32}$$

and it satisfies the Cauchy-Riemann conditions for the differentiation, therefore, substituting (32) into (31) it leads

$$\kappa c^j_p = \delta_{1p} a^j_0 - \overline{a}^j_p + \sum_{k=1}^{\infty o} \eta_{kp} a^j_k + (1-\kappa)\delta_{1p}(\delta_{1\alpha} - i\delta_{2\alpha})R \tag{33}$$

The tangential imperfect parameter is defined in each arc by $K_s(\theta) = K_j, \quad \theta_j < \theta < \theta_{j+1} \quad$ with $\quad j = 0, \ldots, n-1, \quad \theta_0 \equiv 0, \theta_n \equiv 2\pi$, thereby using (16)–(18), the expression (13) yields

$$\left[{}^j u_2 + (x_2\delta_{1\alpha} - x_1\delta_{2\alpha})\right]_{\theta_j}^{\theta_{j+1}} = \int_{\theta_j}^{\theta_{j+1}} K_j\left({}^j u_3^{(1)} - {}^j u_3^{(2)}\right) d\theta \quad \theta_j < \theta < \theta_{j+1}$$

$$\left[\kappa^j u_2 + \kappa(x_2\delta_{1\alpha} - x_1\delta_{2\alpha})\right]_{\theta_j}^{\theta_{j+1}} = \int_{\theta_j}^{\theta_{j+1}} K_j\left({}^j u_3^{(1)} - {}^j u_3^{(2)}\right) d\theta \quad \theta_j < \theta < \theta_{j+1}. \tag{34}$$

The other expression for c^j_p can be derived from (34)

$$\left(\frac{K_j}{p} + \kappa\right) c^j_p = K_j \quad a^j_0 \delta_{1p} + \frac{\overline{a}^j_p}{p} + \sum_{k=1}^{\infty o} \frac{\eta_{kp} a^j_k}{p}\Bigg) - \kappa R \delta_{1p}(\delta_{1\alpha} - i\delta_{2\alpha}) \theta_j < \theta < \theta_{j+1}. \tag{35}$$

Equating the expressions (33) and (35) leads to the infinite system (19).

Appendix B.

Derivation of the effective coefficients given by (29) for the problem $_{13}L$

The integrals from the right side of (27), and (28) are required to be calculated. Therefore, the contributions of each part in the integrals are written as

$$i\int_\Gamma u_3^{(1)} dx_1 = i\sum_{j=0}^{n-1} \int_{\theta_j}^{\theta_{j+1}} {}^{j+1} u_3^{(1)} dx_1, \quad \int_\Gamma u_3^{(1)} dx_2 = \sum_{j=0}^{n-1} \int_{\theta_j}^{\theta_{j+1}} {}^{j+1} u_3^{(1)} dx_2,$$

$$i\int_\Gamma u_3^{(2)} dx_1 = i\sum_{j=0}^{n-1} \int_{\theta_j}^{\theta_{j+1}} {}^{j+1} u_3^{(2)} dx_1, \quad \int_\Gamma u_3^{(2)} dx_2 = \sum_{j=0}^{n-1} \int_{\theta_j}^{\theta_{j+1}} {}^{j+1} u_3^{(2)} dx_2,$$

using the expressions (16), and (17) over the circular contour determined by $z = \mathrm{Re}^{i\theta}$ and the property $\mathrm{Re}(z) = \frac{z+\overline{z}}{2}$ we obtain

$$i\int_\Gamma u_3^{(1)} dx_1 = \frac{i}{2}\sum_{j=0}^{n-1} \int_{\theta_j}^{\theta_{j+1}} \left[\sum_{p=1}^{\infty o} \quad a_0^{j+1}\delta_{1p} + \overline{a}_p^{j+1} + \sum_{k=1}^{\infty o} \eta_{kp} a_k^{j+1}\Bigg) e^{ip\theta} + \sum_{p=1}^{\infty o} \quad \overline{a}_0^{j+1}\delta_{1p} + a_p^{j+1} + \sum_{k=1}^{\infty o} \eta_{kp} \overline{a}_k^{j+1}\Bigg) e^{-ip\theta}\right] dx_1 \tag{36}$$

$$\int_\Gamma u_3^{(1)} dx_2 = \frac{1}{2}\sum_{j=0}^{n-1} \int_{\theta_j}^{\theta_{j+1}} \left[\sum_{p=1}^{\infty o} \quad a_0^{j+1}\delta_{1p} + \overline{a}_p^{j+1} + \sum_{k=1}^{\infty o} \eta_{kp} a_k^{j+1}\Bigg) e^{ip\theta} + \sum_{p=1}^{\infty o} \quad \overline{a}_0^{j+1}\delta_{1p} + a_p^{j+1} + \sum_{k=1}^{\infty o} \eta_{kp} \overline{a}_k^{j+1}\Bigg) e^{-ip\theta}\right] dx_2 \tag{37}$$

$$i\int_\Gamma u_3^{(2)} dx_1 = \frac{i}{2}\sum_{j=0}^{n-1} \int_{\theta_j}^{\theta_{j+1}} \quad \sum_{p=1}^{\infty o} c_p^{j+1} e^{ip\theta} + \sum_{p=1}^{\infty o} \overline{c}_p^{j+1} e^{-ip\theta}\Bigg) dx_1 \tag{38}$$

$$\int_\Gamma u_3^{(2)} dx_2 = \frac{1}{2}\sum_{j=0}^{n-1} \int_{\theta_j}^{\theta_{j+1}} \quad \sum_{p=1}^{\infty o} c_p^{j+1} e^{ip\theta} + \sum_{p=1}^{\infty o} \overline{c}_p^{j+1} e^{-ip\theta}\Bigg) dx_2 \tag{39}$$

Replacing (38) and (39) into the third term of the right side of (27), and (28) and using $dx_2 + idx_1 = Re^{-i\theta} d\theta$ yields $\frac{C^{(2)}_{55}}{V}\left(\int_\Gamma u_3^{(2)} dx_2 + i\int_\Gamma u_3^{(2)} dx_1\right) = \frac{C^{(2)}_{55} R}{2V} \sum_{j=0}^{n-1} \int_{\theta_j}^{\theta_{j+1}} \left(\sum_{p=1}^{\infty o} c_p^{j+1} e^{i(p-1)\theta} + \sum_{p=1}^{\infty o} \overline{c}_p^{j+1} e^{-i(p+1)\theta}\right) d\theta.$

Now, separating the first term of the sum with exponent $(p-1)$ and rearranging the expression

$$\frac{C_{55}^{(2)}}{V}\left(\int_\Gamma u_3^{(2)}dx_2 + i\int_\Gamma u_3^{(2)}dx_1\right) = \frac{C_{55}^{(2)}R}{2V}\sum_{j=0}^{n+1}(\theta_{j+1}-\theta_j)c_1^{j+1} + \frac{C_{55}^{(2)}R}{2V}\sum_{j=0}^{n-1}\int_{\theta_j}^{\theta_{j+1}} \times \sum_{p=3}^{\infty}{}^{o} c_p^{j+1}e^{i(p-1)\theta} + \sum_{p=1}^{\infty}{}^{o}\overline{c}_p^{j+1}e^{-i(p+1)\theta}\Bigg)d\theta \tag{40}$$

Moreover, from the expression (33) we have for $p = 1$

$$c_1^{j+1} = \frac{1}{\kappa}\left[\left(a_0^{j+1} - \overline{a}_1^{j+1} + \sum_{k=1}^{\infty}{}^{o}\eta_{k1}a_k^{j+1}\right) + (1-\kappa)(\delta_{1\alpha} - i\delta_{2\alpha})R\right] \quad \text{if } \theta_j < \theta < \theta_{j+1} \tag{41}$$

Replacing (33) and (41) into (40) for the problem ${}_{13}L$ $(\alpha = 1)$ we have

$$\frac{C_{55}^{(2)}}{V}\left(\int_\Gamma u_3^{(2)}dx_2 + i\int_\Gamma u_3^{(2)}dx_1\right) = \frac{C_{55}^{(1)}R}{2V}\sum_{j=0}^{n-1}\left[a_0^{j+1} - \overline{a}_1^{j+1} + \sum_{k=1}^{\infty}{}^{o}\eta_{k1}a_k^{j+1} + (1-\kappa)R\right](\theta_{j+1}-\theta_j) + \frac{C_{55}^{(1)}R}{2V}\sum_{j=0}^{n-1}\int_{\theta_j}^{\theta_{j+1}}\left\{\sum_{p=1}^{\infty}{}^{o}\left[\delta_{1p}\overline{a}_0^{j+1} - a_p^{j+1} + \sum_{k=1}^{\infty}{}^{o}\overline{\eta}_{kp}\overline{a}_k^{j+1} + (1-\kappa)\delta_{1p}R\right]e^{-i(p+1)\theta} - \sum_{p=3}^{\infty}{}^{o}\ \overline{a}_p^{j+1} - \sum_{k=1}^{\infty}{}^{o}\eta_{kp}a_k^{j+1}\Bigg)e^{i(p-1)\theta}\right\}d\theta \tag{42}$$

Replacing (36) and (37) into the second term of the righ side of (27), and (28) it yields

$$-\frac{C_{55}^{(1)}}{V}\left(\int_\Gamma u_3^{(1)}dx_2 + i\int_\Gamma u_3^{(1)}dx_1\right) = -\frac{C_{55}^{(1)}R}{2V}\sum_{j=0}^{n-1}\int_{\theta_j}^{\theta_{j+1}}\left[\sum_{p=1}^{\infty}{}^{o}\ a_0^{j+1}\delta_{1p} + \overline{a}_p^{j+1} + \sum_{k=1}^{\infty}{}^{o}\eta_{kp}a_k^{j+1}\Bigg)e^{i(p-1)\theta} + \sum_{p=1}^{\infty}{}^{o}\ \overline{a}_0^{j+1}\delta_{1p} + a_p^{j+1} + \sum_{k=1}^{\infty}{}^{o}\eta_{kp}\overline{a}_k^{j+1}\Bigg)e^{-i(p+1)\theta}\right]d\theta.$$

Now, separating the first term of the sum with exponent $(p-1)$ and rearranging the expression

$$-\frac{C_{55}^{(1)}}{V}\left(\int_\Gamma u_3^{(1)}dx_2 + i\int_\Gamma u_3^{(1)}dx_1\right) = -\frac{C_{55}^{(1)}R}{2V}\sum_{j=0}^{n-1}(\theta_{j+1}-\theta_j)\ \ a_0^{j+1} + \overline{a}_1^{j+1} + \sum_{k=1}^{\infty}{}^{o}\eta_{k1}a_k^{j+1}\Bigg) - \frac{C_{55}^{(1)}R}{2V}\sum_{j=0}^{n-1}\int_{\theta_1}^{\theta_2}\left[\sum_{p=3}^{\infty}{}^{o}\ \overline{a}_p^{j+1} + \sum_{k=1}^{\infty}{}^{o}\eta_{kp}a_k^{j+1}\Bigg)e^{i(p-1)\theta} + \sum_{p=1}^{\infty}{}^{o}\ \overline{a}_0^{j+1}\delta_{1p} + a_p^{j+1} + \sum_{k=1}^{\infty}{}^{o}\overline{\eta}_{kp}\overline{a}_k^{j+1}\Bigg)e^{-i(p+1)\theta}\right]d\theta \tag{43}$$

The expressions (42) and (43) are replaced into (27),

$$C_{55}^* - iC_{45}^* = \langle C_{55}\rangle - \frac{C_{55}^{(1)}R}{2V}\sum_{j=0}^{n-1}(\theta_{j+1}-\theta_j)\left[2\overline{a}_1^{j+1} - (1-\kappa)R\right] + \frac{C_{55}^{(1)}R}{2V}\sum_{j=0}^{n-1}\int_{\theta_j}^{\theta_{j+1}}\left\{\sum_{p=1}^{\infty}{}^{o}\left[-2a_1^{j+1} + (1-\kappa)\delta_{1p}R\right]e^{-i(p+1)\theta} - 2\sum_{p=3}^{\infty}{}^{o}\overline{a}_p^{j+1}e^{i(p-1)\theta}\right\}d\theta$$

and using the average definition, the fiber volume fraction $V_2 = \frac{\pi R^2}{V}$, after some algebraic manipulations we obtain

$$C_{55}^* - iC_{45}^* = C_{55}^{(1)}\left[1 - \frac{V_2}{\pi R}\sum_{j=0}^{n-1}(\theta_{j+1}-\theta_j)\overline{a}_1^{j+1}\right] - \frac{C_{55}^{(1)}R}{2V}\sum_{j=0}^{n-1}\left\{\sum_{p=1}^{\infty}{}^{o}\left[2a_p^{j+1} - (1-\kappa)\delta_{1p}R\right] \times e^{-\frac{i(p+1)\theta_j}{2}}e^{-\frac{i(p+1)\theta_{j+1}}{2}}\frac{e^{\frac{i(p+1)\left(\theta_{j+1}-\theta_j\right)}{2}} - e^{-\frac{i(p+1)\left(\theta_{j+1}-\theta_j\right)}{2}}}{i(p+1)} + 2\sum_{p=3}^{\infty}{}^{o}\overline{a}_p^{j+1}e^{\frac{i(p-1)\theta_{j+1}}{2}}e^{\frac{i(p-1)\theta_j}{2}}\frac{e^{\frac{i(p-1)\left(\theta_{j+1}-\theta_j\right)}{2}} - e^{-\frac{i(p-1)\left(\theta_{j+1}-\theta_j\right)}{2}}}{i(p-1)}\right\} \tag{44}$$

The last formula (44) leads to the expression (29). Analogously, the expression (30) for the local problem ${}_{23}L$ is derived.

References

Andrianov, I.V., Danishevs'kyy, V.V., Guillet, A., Pareige, P., 2005. Effective properties and micro-mechanical response of filamentary composite wires under longitudinal shear. Eur. J. Mech. A. Solid 24, 195–206.

Andrianov, I.V., Bolshakov, V.I., Danishevśkyy, V.V., Weichert, D., 2007. Asymptotic simulation of imperfect bonding in periodic fibre-reinforced composite materials under axial shear. Int. J. Mech. Sci. 49, 1344–1354.

Andrianov, I.V., Danishevs'kyy, V.V., Kalamkarov, A.L., 2008. Micromechanical analysis of fiber-reinforced composites on account of influence of fiber coatings. Compos. Part B-Eng. 39, 874–881.

Bakhvalov, N., Panasenko, G.P., 1989. Homogenisation: Averaging Processes in Periodic Media. Kluwer, Dordrecht.

Benveniste, Y., Miloh, T., 2001. Imperfect soft and stiff interfaces in two dimensional elasticity. Mech. Mater. 33, 309–323.

Camacho-Montes, H., Sabina, F.J., Bravo-Castillero, J., Guinovart-Díaz, R., Rodríguez-Ramos, R., 2009. Magnetoelectric coupling and cross-property connections in a square array of a binary composite. Int. J. Eng. Sci. 47, 294–312.

Craus, J., Ishai, I., Sides, A., 1978. Some physico-chemical aspects of the effect and the role of the filler in bituminous paving mixtures. J. Assoc. Asphalt Paving Technol., 47558–47588.

Garboczi, E.J., Bentz, D.P., 1997. Analytical formulas for interfacial transition zone properties. Adv. Cem. Based Mater. 6, 99–108.

Garboczi, E.J., Berryman, J.G., 2000. New effective medium theory for the diffusivity or conductivity of a multi-scale concrete microstructure model. Concr. Sci. Eng. 2, 88–96.

Goland, M., Reissner, E., 1944. The stresses in cemented joints. J. Appl. Mech. 11, 17–27.

Guinovart-Díaz, R., Yan, P., Rodríguez-Ramos, R., López-Realpozo, J.C., Jiang, C.P., Bravo-Castillero, J., Sabina, F.J., 2012. Effective properties of piezoelectric composites with parallelogram periodic cells. Int. J. Eng. Sci. 53, 58–66.

Guinovart-Díaz, R., Rodríguez-Ramos, R., Bravo-Castillero, J., López-Realpozo, J.C., Sabina, F.J., Sevostianov, I., 2013. Effective elastic properties of a periodic fiber reinforced composite with parallelogram-like arrangement of fibers and imperfect contact between matrix and fibers. Int. J. Solids Struct. 50, 2022–2032.

Hashin, Z., 1990. Thermoelastic properties of fiber composites with imperfect interface. Mech. Mater. 8, 333–338.

Hashin, Z., 1991a. The spherical inclusion with imperfect interface. J. Appl. Mech. 58, 444–449.

Hashin, Z., 1991b. Thermoelastic properties of particulate composites with imperfect interface. J. Mech. Phys. Solids 39, 745–762.

Hashin, Z., 2002. Thin interphase/imperfect interface in elasticity with application to coated fiber composites. J. Mech. Phys. Solids 50, 2509–2537.

Jiang, C.P., Xu, Y.L., Cheung, Y.K., Lo, S.H., 2004. A rigorous analytical method for doubly periodic cylindrical inclusions under longitudinal shear and its application. Mech. Mater. 36, 225–237.

Kanaun, S.K., Kudriavtseva, L.T., 1983. Spherically layered inclusions in a homogeneous elastic medium. Appl. Math. Mech. 50, 483–491.

Kanaun, S.K., Kudriavtseva, L.T., 1986. Elastic and thermoelastic characteristics of composites reinforced with unidirectional fibre layers. Appl. Math. Mech. 53, 628–636.

Kantarovich, L.V., Krylov, V.I., 1964. Approximate Methods of Higher Analysis, Interscience Publishers, INC-New York, P. Noordhoff LTD-Groningen, The Netherlands.

Lopez-Lopez, E., Sabina, F.J., Bravo-Castillero, J., Guinovart-Díaz, R., Rodríguez-Ramos, R., 2005. Overall electromechanical properties of a binary composite with 622 symmetry constituents. Antiplane shear piezoelectric state. Int. J. Solids Struct. 42, 5765–5777.

Lopez-Realpozo, J.C., Rodriguez-Ramos, R., Guinovart-Diaz, R., Bravo-Castillero, J., Sabina, F.J., 2011. Transport properties in fibrous elastic rhombic composite with imperfect contact condition. Int. J. Mech. Sci. 53, 98–107.

Mahiou, H., Beakou, A., 1998. Modelling of interfacial effects on the mechanical properties of fibre-reinforced composites. Compos. Part A 29A, 1035–1048.

Molkov, B.A., Pobedria, B.E., 1985. Effective characteristic of fibrous unidirectional composite with periodic structure. Mech. Solids 2, 119–129 (in Russian).

Molkov, B.A., Pobedria, B.E., 1988. Effective elastic properties of a composite with elastic contact. Izvestia Akademia Nauk SSR Mekanika Tverdovo Tela 1, 111–117 (in Russian).

Movchan, A.B., Movchan, N.V., Poulton, C.G., 2002. Asymptotic Models of Fields in Dilute and Densely Packed Composites. Imperial College Press, London.

Muskhelishvili, N.I., 1953. Some Basic Problems in the Mathematical Theory of Elasticity. Noordhoff, Groningen.

Pobedria, B.E., 1984. Mechanics of Composite Materials. Moscow State University Press, Moscow (in Russian).

Rodriguez-Ramos, R., Sabina, F.J., Guinovart-Díaz, R., Bravo-Castillero, J., 2001. Closed form expressions for the effective coefficients of fibre-reinforced composite with transversely isotropic constituents – I. Elastic and square symmetry.. Mech. Mater. 33, 223–235.

Rodriguez-Ramos, R., Yan, P., Lopez-Realpozo, J.C., Guinovart-Díaz, R., Bravo-Castillero, J., Sabina, F.J., Jiang, C.P., 2011. Two analytical models for the study of periodic fibrous elastic composite with different unit cells. Compos. Struct. 93, 709–714.

Rodriguez-Ramos, R., Berger, H., Guinovart-Díaz, R., López-Realpozo, J.C., Würkner, M., Gabbert, U., Bravo-Castillero, J., 2012. Two approaches for the evaluation of the effective properties of elastic composite with parallelogram periodic cells. Int. J. Eng. Sci. 58, 2–10.

Sevostianov, I., 2007. Dependence of the effective thermal pressure coefficient of a particulate composite on particles size. Int. J. Fract. 145, 333–340.

Sevostianov, I., Kachanov, M., 2007. Effect of interphase layers on the overall elastic and conductive properties of matrix composites. Applications to nanosize inclusion. Int. J. Solids Struct. 44, 1304–1315.

Sevostianov, I., Sabina, F., 2007. Cross-property connections for fiber reinforced piezoelectric materials. Int. J. Eng. Sci. 45, 719–735.

Sevostianov, I., Sabina, F.J., Bravo-Castillero, J., Guinovart-Diaz, R., Rodriguez-Ramos, R., 2006. Cross-property connections for fiber-reinforced composites with transversely-isotropic constituents. Int. J. Fract. 142, 299–306.

Sevostianov, I., Rodríguez-Ramos, R., Guinovart-Díaz, R., Bravo-Castillero, J., Sabina, F.J., 2012. Connections between different models describing imperfect interfaces in periodic fiber-reinforced composites. Int. J. Solids Struct. 49, 1518–1525.

Shen, L., Li, J., 2003. Effective elastic moduli of composites reinforced by particle or fiber with an inhomogeneous interface. Int. J. Solids Struct. 40, 1393–1409.

Shen, L., Li, J., 2005. Homogenization of a fibre/sphere with an inhomogeneous interphase for the effective elastic moduli of composites. Proc. R. Soc. London, A 461, 1475–1504.

Wang, W., Jasiuk, I., 1998. Effective elastic constants of particulate composites with inhomogeneous interphases. J. Compos. Mater. 32, 1391–1424.

Wang, J., Duan, H.L., Zhang, Z., Huang, Z.P., 2005. An anti-interpenetration model and connections between interphase and interface models in particle reinforced composites. Int. J. Eng. Sci. 47, 701–718.

Zhu, Xing-yi., Yang, Zhong-xuan., Guo, Xing-ming., Chen, Wei-qiu., 2011. Modulus prediction of asphalt concrete with imperfect bonding between aggregate–asphalt mastic. Compos. Part B-Eng. 42, 1404–1411.